

Application of Vis/NIR spectroscopy for the estimation of soluble solids, dry matter and flesh firmness in stone fruits

Journal:	<i>Journal of the Science of Food and Agriculture</i>
Manuscript ID	JSFA-20-2849
Wiley - Manuscript type:	Research Article
Date Submitted by the Author:	13-Jul-2020
Complete List of Authors:	Scalisi, Alessio; Agriculture Victoria, Department of Jobs, Precincts and Regions O'Connell, Mark; Agriculture Victoria, Department of Jobs, Precincts and Regions
Key Words:	apricot, fruit quality, near-infrared, nectarine, peach, plum

SCHOLARONE™
Manuscripts

1
2
3 1 **Application of Vis/NIR spectroscopy for the estimation of soluble solids, dry matter and**
4
5 2 **flesh firmness in stone fruits**

6
7
8 3
9
10 4 **Running title:** Use of near-infrared (NIR) absorbance to assess stone fruit quality parameters.
11
12 5

13
14 6 **Alessio Scalisi*, Mark Glenn O'Connell**

15
16
17 7 Agriculture Victoria, Department of Jobs, Precincts and Regions, 255 Ferguson Road, Tatura,
18
19 8 VIC, 3616, Australia

20
21 9
22
23
24 10 * Corresponding author (E-mail: alessio.scalisi@ecodev.vic.gov.au)
25

26
27
28 12 **Abstract**

29
30 13 **BACKGROUND:** Soluble solids concentration (SSC), dry matter concentration (DMC)
31
32
33 14 **and flesh firmness (FF) are important fruit quality parameters in stone fruits. This study**
34
35 15 **investigated the ability of a commercial Vis/NIR spectrometer to determine SSC, DMC**
36
37 16 **and FF in nectarine, peach, apricot and Japanese plum cultivars at harvest. The work**
38
39 17 **was conducted in summer 2019/20 on fourteen stone fruit cultivars at Tatura, Australia.**
40
41 18 **Two sub-samples of 100 fruit each were collected before and after commercial maturity**
42
43 19 **(± 5 days) in order to maximise sample variability.**

44
45
46 20 **RESULTS:** Partial least square regression (PLS) models based on the 2nd derivative of
47
48 21 **the absorbance in the 729–975 nm spectral region proved accurate for the prediction of**
49
50 22 **SSC and DMC ($R^2_{CV} > 0.750$). Only the model generated for SSC in 'Golden May' apricot**
51
52 23 **was less precise compared to other cultivars. No Vis/NIR models were accurate enough**
53
54 24 **to predict FF in the cultivars under study ($R^2_{CV} < 0.750$).**
55
56
57
58
59
60

1
2
3 25 **CONCLUSION: This study demonstrated that the Vis/NIR spectrometer was a reliable**
4
5 26 **tool to monitor SSC and DMC in stone fruits at harvest but proved less useful for FF**
6
7 27 **estimation. These results highlight the potential of Vis/NIR spectrometry to evaluate**
8
9 28 **stone fruit quality both *in situ* pre-harvest and in the laboratory after harvest.**

10
11
12 29
13
14 30 **Keywords:** apricot; fruit quality; near-infrared; nectarine; peach; plum

15
16
17 31
18
19 32 **1. Introduction**

20
21 33 Portable, rapid, non-destructive devices for the determination of objective fruit quality
22
23 34 parameters offer improvements over traditional destructive and labour-expensive approaches
24
25 35 to guide harvesting and marketing operations and supply chain logistics. Quality parameters
26
27 36 provide insightful information on the ripening stage of specific fruit crops, and based on the
28
29 37 traditional reference maturity indices, technology can be adapted for the estimation of fruit
30
31 38 maturity. For temperate tree fruits, traditionally, sugars, dry matter, flesh firmness, starch,
32
33 39 acidity, colour, size and shape, ethylene production and respiration rate have provided common
34
35 40 indicators of maturity. Each fruit and/or cultivar has key maturity indices based on its genetic,
36
37 41 morphological and physiological characteristics, or a combination. In stone fruit, several
38
39 42 maturation indices can be used to determine the best harvest time. Maximising sugars,
40
41 43 specifically soluble solids concentration (SSC), is a strategy of some fruit growers to improve
42
43 44 quality and to determine harvest time. Flesh firmness (FF) is commonly used in apricot,
44
45 45 nectarine, peach and plum as an indicator of ripeness.¹ However, a high degree of variability
46
47 46 in SSC and FF is found among different cultivars^{2, 3} making them not universal parameters for
48
49 47 stone fruit maturity assessment, if used alone. Dry matter concentration (DMC) has been
50
51 48 efficiently used to determine maturity in crops that accumulate oil in their fruit such as
52
53
54
55
56
57
58
59
60

1
2
3 49 avocado⁴ and olive,⁵ and more recently for quality determination in mango,⁶ kiwifruit,⁷ apple⁸
4
5 50 and cherry.⁹
6
7

8 51 Besides being used as maturity indices, SSC, FF and DMC can be determined prior to
9
10 52 harvest as quality parameters to anticipate the marketability of the produce and to improve
11
12 53 harvest logistics. Typical SSC, FF and DMC determination requires sample destruction and
13
14 54 can be expensive as specific equipment and labour are required. Therefore, a non-destructive
15
16 55 device that can accurately predict multiple fruit quality parameters is highly sought after by
17
18 56 industry. Visible/Near Infrared (Vis/NIR) spectrometry is one of the most established non-
19
20 57 destructive technology for the prediction of several quality and maturity indicators in temperate
21
22 58 fruit crops and has been successfully used in apple,^{10,11} stone fruits,^{12,13,14,15} pear^{16,17} and several
23
24 59 other crops. Many commercial in-line grader systems come fully equipped with near infrared
25
26 60 spectrometers that quickly assess quality parameters after harvest¹⁸, but there is a need to assess
27
28 61 the usefulness of Vis/NIR spectrometers for field and laboratory monitoring of stone fruit
29
30 62 quality indices. Golic and Walsh validated the suitability of NIR spectroscopy in commercial
31
32 63 graders to estimate SSC in stone fruits.¹⁹ A range of handheld NIR devices is currently
33
34 64 commercially available and their performance for the estimation of fruit DMC was compared
35
36 65 by Kaur *et al.*²⁰. Donis-González *et al.* compared two portable devices for the estimation of
37
38 66 SSC and DMC in peach, finding an overall better ability to predict the latter, and a reduced
39
40 67 estimation power for the former.²¹
41
42
43
44
45

46 68 With the goal of improving harvest logistics and labour efficiency, this study aimed to
47
48 69 investigate the suitability of a portable Vis/NIR spectrometer as a smart tool for the estimation
49
50 70 of SSC, DMC and FF in nectarine, peach, apricot and Japanese plum cultivars at harvest.
51
52
53
54
55

56 72 **MATERIALS AND METHODS**

57 73 **Experimental site and cultivar characteristics**

1
2
3 74 The experiment was carried out in the summer of 2019/20 in a stone fruit orchard at the
4
5 75 Tatura SmartFarm, Agriculture Victoria, Australia (36°26'7" S and 145°16'8" E, 113 m a.s.l.).
6
7
8 76 The stone fruit orchard (3.0 ha) at the farm comprises agronomic experiments on apricot,
9
10 77 nectarine, peach and plum. A total of fourteen cultivars, i.e. one apricot (*Prunus armeniaca* L.,
11
12 78 'Golden May'), one Japanese plum (*P. salicina* L., 'Angeleno'), four nectarine (*P. persica* L.
13
14 79 Batsch, 'August Bright', 'Autumn Bright', 'Rose Bright' and 'September Bright'), four yellow
15
16 80 peach (*P. persica* L. Batsch, 'August Flame', late 'O'Henry', 'Redhaven' and 'September Sun')
17
18 81 and four white peach (*P. persica* L. Batsch, 'Ice Princess', 'Snow Fall', 'Snow Flame 23' and
19
20 82 'Snow Flame 25') were selected for this study. The harvest time of all the cultivars stretched
21
22 83 from December 2019 to April 2020, with the first to reach commercial maturity being the
23
24 84 apricot 'Golden May' (i.e. early December), and the last being the white peach 'Snow Fall' (i.e.
25
26 85 start of April). The orchard was planted in 2013–2015, the soil had a clay loam soil texture and
27
28 86 trees were irrigated, fertigated, thinned, pest/disease-managed and pruned based on
29
30 87 commercial practices.
31
32
33
34
35
36
37

38 89 **Fruit sampling and preparation**

39
40 90 Fruit from each cultivar were collected at two different times, one slightly before (1st batch)
41
42 91 and one slightly after commercial harvest (2nd batch), within a window of ten days. Each batch
43
44 92 of fruit included specimens with diverse size and colour. This sample collection method was
45
46 93 applied to target fruit at different maturity stages and increase sample variability. Commercial
47
48 94 harvest time was assessed by a DA-meter (TR Turoni, Forli, Italy) based on the index of
49
50 95 absorbance difference (I_{AD}) thresholds provided by the HIN (Victorian Horticulture Industry
51
52 96 Network).²² The only exception occurred for 'Redhaven', of which the two batches of fruit were
53
54 97 harvested after commercial harvest because the DA-meter was temporarily unavailable. Each
55
56 98 batch of fruit consisted of 100 fruit, leading to a total sample size of 200 fruit for each of the
57
58
59
60

1
2
3 99 fourteen cultivars collected over a total of 28 days of measurements between December 2019
4
5 100 and April 2020.

6
7 101 Fruit were harvested in the early morning from different canopy sides and heights (i.e. to
8
9 102 pool together fruit that received different amounts of sunlight), immediately brought to the
10
11 103 laboratory, numbered and weighed, and then left on the laboratory bench for two hours in order
12
13 104 to adjust to a standard temperature of 25 °C prior to measurement.
14
15

16
17 105

18 19 106 **Vis/NIR spectrometry**

20
21 107 In this study we used a commercial portable F-750 Produce Quality Meter (Felix
22
23 108 Instruments, Camas, WA, USA) for Vis/NIR spectra collections in the 310–1100 nm range
24
25 109 with a resolution of 3 nm. This device is equipped with a Carl Zeiss MMC-1 spectrometer, a
26
27 110 xenon tungsten lamp as light source and a glass coated lens as per manufacturer specifications.
28
29

30
31 111 A circular area ($\approx \text{Ø } 30 \text{ mm}$) was marked on a single side of each fruit and scanned using
32
33 112 the F-750 meter. Each batch of 100 fruit was scanned within one hour after samples had reached
34
35 113 25 °C in the same morning after fruit collection. The device recorded the absorbance spectra
36
37 114 and their second derivatives, which were subsequently smoothed using a Savitzky and Golay
38
39 115 10-point convolution. Data were stored in an SD card and downloaded prior to data analysis.
40
41

42 116

43 44 117 **Reference destructive determinations**

45
46 118 Once spectra were collected, the fruit were immediately destructed for SSC, DMC and FF
47
48 119 determination. Fruit skin was peeled off from the area previously scanned with the F-750 meter,
49
50 120 and flesh was exposed to a penetrometer (FT327, FACCHINI srl, Alfonsine, Italy) equipped
51
52 121 with an 8 mm tip to measure FF on a scale from 0 to 15 kgf. Afterwards, a few drops of juice
53
54 122 were extracted with the help of a pointy tool and SSC was measured using a digital
55
56 123 refractometer (PR-1; ATAGO CO., LTD, Saitama, Japan) and expressed as °Brix. After SSC
57
58
59
60

1
2
3 124 determination, a cylindrical core ($\varnothing \approx 30$ mm, $h \approx 15$ mm) of the pulp — where previous
4
5 125 measurements were taken — was extracted using a fruit corer and weighed on a digital scale
6
7 126 with four decimal places. Fresh mass was instantly recorded, cores were placed in silicone trays
8
9 127 and dried in an oven at 55 °C until constant weight was obtained (≈ 72 –96 h). Afterwards,
10
11 128 samples were weighed to determine dry mass and DMC (%) was calculated as dry mass / fresh
12
13 129 mass $\times 100$.
14
15
16
17 130

19 131 **Data analysis and prediction models**

21 132 Fruit fresh weight (FW), SSC, FF and DMC were represented using boxplots to determine
22
23 133 average values and sample variability for each cultivar. Collected Vis/NIR spectra were
24
25 134 analysed with a partial least square regression (PLS) procedure using Minitab® Statistical
26
27 135 Software (Minitab, LL v.19, PA, USA). The absorbance spectra between 729 and 975 nm and
28
29 136 their second derivatives were tested and compared in terms of robustness of the prediction
30
31 137 models for SSC, DMC and FF. The region between 729 and 975 nm was chosen as it has
32
33 138 previously been linked to sugars, carbohydrate and water absorbance.^{9,10,17} For comparison
34
35 139 purposes, secondary FF models were built using the 500–1000 nm spectral region, in
36
37 140 accordance with the wavelengths used by Uwadaira *et al.* for FF estimation in peach.²³ The
38
39 141 PLS procedure used the nonlinear iterative partial least squares (NIPALS) algorithm and
40
41 142 consisted of three steps. First, a train-sample composed of 170 fruit per cultivar (minus
42
43 143 measurement errors and/or outliers in the sample) was used to generate the prediction model.
44
45 144 A second step was carried out by performing a leave-one-out (LOO) cross-validation (CV) on
46
47 145 the same sample. The third and last step consisted of testing model robustness on 30 additional
48
49 146 fruit per cultivar (test-sample). Half of the 30 test-sample fruit originated from the 1st batch and
50
51 147 the other half from the 2nd batch of harvested fruit. Model robustness was determined based on
52
53 148 the number of principal components (PCs), the coefficient of determination of the model (R^2)
54
55
56
57
58
59
60

1
2
3 149 and the root mean square error (*RMSE*) calculated as the standard deviation of the residuals
4
5 150 and expressed with the same units of each variable (i.e. °Brix for SSC, % for DMC and kgf for
6
7
8 151 FF). The R^2 and *RMSE* were calculated for the prediction model and for the CV (R^2_{CV} and
9
10 152 $RMSE_{CV}$, respectively) using from 1 to 10 PCs. In short, preferable models had fewer PCs, high
11
12 153 R^2 and low *RMSE*. The best models for each cultivar were selected by looking at the lowest
13
14 154 number of PCs used for R^2_{CV} and $RMSE_{CV}$ to reach values near their maximum and minimum,
15
16 155 respectively. Once models were selected, the second step consisted of validating them on the
17
18
19 156 test-sample and expressing their accuracy by comparing the test R^2 (R^2_{test}) to the R^2_{CV} . A large
20
21 157 difference between the two coefficients indicated low predictive ability for an external sample.
22
23
24 158 Although frequently used in PLS model comparison, the ratio of performance to deviation (i.e.
25
26 159 RPD or residual prediction deviation) was not considered as a measure of goodness of fit in
27
28 160 this study, as it is redundant with the use of R^2_{CV} ,²⁴ and less known in the scientific community,
29
30 161 making it difficult to be correctly interpreted.
31
32
33 162

35 163 RESULTS AND DISCUSSION

37 164 Fruit characteristics

38 165 Boxplots in Fig. 1 show variability and sample characteristics of FW, SSC, FF and DMC
39
40 166 for each cultivar under study. FW provided an indication of fruit size. 'Golden May' apricot
41
42 167 and 'Angeleno' plum trees yielded the smallest fruit and had uniform size, with means \pm
43
44 168 standard deviations equal to 46.26 ± 13.10 g and 67.33 ± 12.02 g, respectively, whereas
45
46 169 'September Sun' and 'Snow Fall' produced the largest fruit (192.94 ± 54.18 g and $174.41 \pm$
47
48 170 57.09 g, respectively), but also had less homogenous FW (Fig. 1A). On the one hand,
49
50 171 'Angeleno' plums had the highest SSC with very low variability among fruits (19.69 ± 1.35
51
52 172 °Brix). On the other hand, 'Golden May' apricots expressed a very large SSC variability (Fig.
53
54 173 1B). 'Redhaven' peach had the lowest FF (2.34 ± 1.52 kgf), followed by 'Angeleno' plum (2.97

174 ± 0.50 kgf), with the former being affected by the late sample collection (Fig. 1C). Overall, FF
175 was characterised by high intra-cultivar variability, except for 'Angeleno' plums that showed a
176 very narrow distribution. DMC had low intra- and inter-cultivar variability, with only
177 'Angeleno' plums expressing a distinctively high mean DMC of 19.44 ± 1.36 % (Fig. 1D).

178

179 **Model analysis and prediction ability**

180 Outliers observed in the distribution analysis (Fig. 1) and erroneous device measurements
181 (i.e. showing false spectra responses) were removed from the samples before building the PLS
182 models. A graphical example of the methodology used for model selection is presented for the
183 estimation of SSC in late 'O'Henry' (Fig. 2). Both the models that used Vis/NIR absorbance
184 (Fig. 2A and C) and its 2nd derivative (Fig. 2B and D) yielded very high R^2 and R^2_{CV} with very
185 small $RMSE$ and $RMSE_{CV}$. However, the latter needed a lower number of PCs than the former.
186 In the case of SSC in 'O'Henry', the most accurate model was built using 4 PCs that summarised
187 the 2nd derivative of the absorbance in the 729–975 nm wavelength. The proximity of model
188 and cross-validation lines in Fig. 2 indicated that the cross-validation efficiently reproduced
189 the prediction model and kept a small prediction error ($RMSE$).

190 In line with what was observed for the prediction of SSC in 'O'Henry', when the absorbance
191 and its 2nd derivative were compared for all the parameters (SSC, DMC and FF) and in all the
192 cultivars under study, they both yielded very similar models, with the exception that the latter
193 always needed less PCs to build the optimal models (3–5) when compared to the former (5–
194 10).

195 In addition, FF models were similar for both the 729–975 and 500–1000 nm regions in terms
196 of R^2 , R^2_{CV} , $RMSE$ and $RMSE_{CV}$ (data not shown). Therefore, only models based on the 2nd
197 derivative of the 729–975 nm absorbance were considered for the following results on SSC,
198 DMC and FF.

1
2
3 199 Model and cross-validation fits for SSC, DMC and FF were plotted against the actual
4
5 200 responses to graphically assess model linearity (Fig. 3, 4 and 5) and data dispersion. In the case
6
7 201 of SSC, model fits responded linearly to actual values and the points were tightly distributed
8
9 202 around the $y = x$ regression line, except for 'Golden May', whose fits were uniformly scattered
10
11 203 farther away (Fig. 3) from the line. This was likely to be due to the high variability of SSC
12
13 204 values highlighted in Fig. 1B. Similar results were obtained for DMC (Fig. 4), although in this
14
15 205 case, model fits in 'Golden May' had a tighter linearity with actual responses than for SSC, as
16
17 206 foreseeable from the lower variability of DMC observed in Fig. 1D. FF responses of model fits
18
19 207 to actual responses were rather erratic (Fig. 5), with high point dispersion in all the cultivars,
20
21 208 suggesting that the absorbance in the 729–975 nm spectra poorly predicts FF in stone fruit.
22
23 209 Cross-validation fits showed almost identical responses to actual responses (Fig. 3, 4 and 5), in
24
25 210 line with the model fits, thus, providing a promising indication of model robustness.

26
27 211 To confirm model linearity and assumptions from observations in Figs. 3–5, $RMSE$,
28
29 212 $RMSE_{CV}$, R^2 and R^2_{CV} were analysed (Table 1). For all the cultivars, $RMSE_{CV}$ was always higher
30
31 213 than $RMSE$, as expected, but the difference between the two errors was very small for all the
32
33 214 observed parameters (< 0.13 °Brix for SSC, < 0.10 % for DMC and < 0.13 kgf for FF).
34
35 215 Similarly, R^2 was expectedly higher than R^2_{CV} but the delta between them was negligible ($<$
36
37 216 0.04 for SSC and DM and < 0.09 for FF). However, assuming a threshold of $R^2_{CV} = 0.75$ —
38
39 217 equivalent to $RPD = 2$, a common threshold of goodness of fit²⁴ — prediction efficiency was
40
41 218 consistently high for SSC and DMC models, but always low for FF models (Table 1). The only
42
43 219 exception occurred for SSC prediction in 'Golden May' apricot, whose model generated a lower
44
45 220 prediction ability ($R^2_{CV} = 0.688$), as foreseen from the preliminary observations in Fig. 3.
46
47 221 Overall, the best prediction models for SSC were obtained for 'August Bright' nectarine and
48
49 222 'August Flame' peach, whereas the most accurate DMC estimation was found in 'September
50
51 223 Sun' and 'Ice Princess' peaches (Table 1). The SSC and DMC models with lowest R^2_{CV} were
52
53
54
55
56
57
58
59
60

224 found in 'Golden May' apricot, followed by 'Redhaven' peach. The low R^2_{CV} found in
225 'Redhaven' might have been influenced by late fruit sampling that led to slightly overripened
226 fruit. As mentioned above, none of the models robustly predicted actual FF responses,
227 regardless of sample variability. Indeed, the two lowest R^2_{CV} were found in 'Angeleno' plum
228 and in 'Ice Princess' peach (Table 1), which had very different sample variabilities (Fig. 1C).

229 Model validation on the further test-sample (i.e. 30 fruit) corroborated model robustness for
230 SSC and DMC in all the cultivars (Table 1). Indeed, R^2_{test} was always very similar to R^2_{CV}
231 (Table 1), with the highest delta (0.134) obtained in the DMC model for 'Ice Princess' peach.
232 In the case of FF, given that R^2_{CV} was always low, it was not needed to further test the model
233 on the test-sample, as there was enough evidence of poor robustness. However, R^2_{test} of FF
234 models are reported in Table 1 for completeness.

235 A first preliminary analysis could lead to associating poor Vis/NIR prediction ability to high
236 sample variability. Nevertheless, models built on accurate readings would benefit from high
237 sample variability if spectra were truly related to specific variables (i.e. sugars, water, etc.).
238 Indeed, very poor prediction ability was obtained for FF in 'Angeleno' plums (R^2 and $R^2_{CV} <$
239 0.30), probably due to highly homogenous FF, in line with previous findings on the same
240 cultivar,²⁵ suggesting that there is likely a physiological explanation that justifies the lack of
241 accuracy for FF prediction. The strong association between NIR spectra and SSC and DMC
242 found in peach is not in line with the findings of Donis-González *et al.*, who observed poor
243 SSC prediction.²¹ This was likely to be due to different sample characteristics (e.g. size and
244 cultivars) and post-harvest handling (i.e. fruit stored at 0 °C after harvest in Donis-González *et*
245 *al.*²¹) as very low temperatures might significantly alter SSC and FF.²⁶ Other studies have
246 successfully predicted SSC and DMC using Vis/NIR wavelengths like the one used in this
247 work (i.e. 729–975 nm).^{9,10,17} The spectral region between 880 and 970 nm was particularly
248 useful for DMC estimation in pear²⁷ since it contains the absorbance bands of starch, cellulose,

1
2
3 249 sucrose and water. FF is influenced by cell wall degradation, which is in turn regulated by
4
5 250 organic acids, pectins and water content.²³ Fruit may also soften due to the indirect effect of
6
7
8 251 external impacts (wind, sunburn, insects, birds and pathogens) that trigger internal biochemical
9
10 252 changes. This multitude of factors affect FF in a combined way, though not unique, meaning
11
12 253 that, for example, while one fruit might mainly soften up due to cell water content changes, the
13
14 254 FF of a second fruit might be lower because of a sudden pest or pathogen occurrence, and a
15
16
17 255 third because of high light exposure and sunburn. Therefore, it is particularly hard to estimate
18
19 256 FF using a predefined combination of the absorbance at different wavelengths. The fact that
20
21 257 Udawaira *et al.* obtained a more robust model to predict FF in the peach 'Akatsuki' ²³ was
22
23 258 probably due to the different sample characteristics, as they used a lower amount of fruit and
24
25
26 259 they progressively ripened fruit post-harvest. Indeed, there might be a significant increase of
27
28 260 FF prediction ability in overripening peach, as indicated by the highest R^2_{CV} observed in
29
30 261 'Redhaven' (Table 1), the only cultivar that was harvested later than commercial maturity.
31
32
33 262 Nonetheless, post-harvest experiments on the same cultivars should be conducted to verify this
34
35 263 assumption.

36
37 264 The models built for all the cultivars proved robust for the estimation of SSC and DMC,
38
39 265 even in the case of the late harvested 'Redhaven', indicating that these two parameters can be
40
41 266 estimated with Vis/NIR spectrometers before and after 'commercial harvest' with a high degree
42
43
44 267 of confidence. However, the R^2_{cv} of SSC and DMC in 'Redhaven' was lower than other
45
46 268 peaches, suggesting that an optimal prediction of these two parameters becomes more difficult
47
48 269 as fruit reach and exceed physiological maturity. The prediction of SSC in 'Golden May' apricot
49
50 270 was not as accurate as for the other stone fruit and further studies on other apricot cultivars
51
52
53 271 need to be conducted to determine if this strictly depends on genotype characteristics and sugar
54
55 272 variability among fruits.

56
57
58 273
59
60

274 CONCLUSIONS

275 Overall, we demonstrated that Vis/NIR can be a reliable tool to monitor SSC and DMC in
276 stone fruits at harvest. This study showed that the 2nd derivative of the absorbance in the 729–
277 975 nm spectral region generated robust models for SSC and DMC. The influence of
278 temperature on Vis/NIR spectra is well known, thus the models in this study are suitable for
279 measurements carried out at temperatures close to the one used in this study (25 °C). However,
280 Vis/NIR spectrometry appears to be not accurate enough for FF determinations in stone fruits
281 and the use of a more direct physical non-destructive method would be advisable (e.g. impact,
282 acoustic or vibration sensors). Based on findings in this study, the Felix F-750 portable device
283 offers the potential for the industry to routinely and rapidly take non-destructive field
284 measurements of SSC and DMC in apricots, Japanese plum, peach and nectarine to improve
285 harvest timing, determine destination markets and match consumers' expectations.

287 ACKNOWLEDGEMENTS

288 The technical support and assistance of Madeleine Peavey, Madita Lauer, Dave Haberfield,
289 and Cameron O'Connell, and the scientific feedback of Dario Stefanelli are gratefully
290 acknowledged. This work was supported by projects 'Horticulture Development Plan Task 1:
291 Yield and quality relationships with light interception' funded by the Victorian Government's
292 Agriculture Infrastructure and Jobs Fund and 'SF17006: Summerfruit orchard — phase II'
293 funded by Hort Innovation using the Summerfruit levy and funds from the Australian
294 Government with co-investment from Agriculture Victoria.

296 REFERENCES

- 297 1 Crisosto CH, Stone fruit maturity indices: a descriptive review. *Postharvest News and*
298 *Information* 5(6): 65N-68N (1994).

- 1
2
3 299 2 Byrne DH, Nikolic AN and Burns EE, Variability in sugars, acids, firmness, and color
4
5 300 characteristics of 12 peach genotypes. *J Amer Soc Hort Sci* **116**: 1004-1006 (1991).
6
7 301 <https://doi.org/10.21273/jashs.116.6.1004>
8
9
10 302 3 Lopresti J, Goodwin I, McGlasson B, Holford P and Golding J. Variability in size and
11
12 303 soluble solids concentration in peaches and nectarines, in *Horticultural Reviews*, ed. by
13
14 304 Janick J, 42 pp. 253-312 (2014). <https://doi.org/10.1002/9781118916827.ch05>
15
16
17 305 4 Lee SK, Young RE, Schiffman PM and Coggins CW. Maturity studies of avocado fruit
18
19 306 based on picking dates and dry weight. *J Amer Soc Hort Sci* **108**: 390-394 (1983).
20
21 307 5 Mickelbart MV and James D, Development of a dry matter maturity index for olive
22
23 308 (*Olea europaea*). *New Zeal J Crop Hort Sci* **31**: 269-276 (2003).
24
25 309 <https://doi.org/10.1080/01140671.2003.9514261>
26
27
28 310 6 Subedi PP, Walsh KB and Owens G, Prediction of mango eating quality at harvest using
29
30 311 short-wave near infrared spectrometry. *Postharvest Biol Tec* **43**: 326-334 (2007).
31
32 312 <https://doi.org/10.1016/j.postharvbio.2006.09.012>
33
34
35 313 7 Harker FR, Carr BT, Lenjo M, MacRae EA, Wismer WV, Marsh KB, Williams M,
36
37 314 White A, Lund CM, Walker SB, Gunson FA and Pereira RB, Consumer liking for
38
39 315 kiwifruit flavour: A meta-analysis of five studies on fruit quality. *Food Qual Prefer* **20**:
40
41 316 30-41 (2009). <https://doi.org/10.1016/j.foodqual.2008.07.001>
42
43
44 317 8 Palmer JW, Harker FR, Tustin DS and Johnston J, Fruit dry matter concentration: a
45
46 318 new quality metric for apples. *J Sci Food Agric* **90**: 2586-2594 (2010).
47
48 319 <https://doi.org/10.1002/jsfa.4125>
49
50
51 320 9 Escribano S, Biasi WV, Lerud R, Slaughter DC and Mitcham EJ, Non-destructive
52
53 321 prediction of soluble solids and dry matter content using NIR spectroscopy and its
54
55 322 relationship with sensory quality in sweet cherries. *Postharvest Biol Tec* **128**: 112-120
56
57 323 (2017). <https://doi.org/10.1016/j.postharvbio.2017.01.016>
58
59
60

- 1
2
3 324 10 McGlone VA, Jordan RB and Martinsen PJ, Vis/NIR estimation at harvest of pre- and
4
5 325 post-storage quality indices for 'Royal Gala' apple. *Postharvest Biol Tec* **25**: 135-144
6
7 326 (2002). [https://doi.org/10.1016/s0925-5214\(01\)00180-6](https://doi.org/10.1016/s0925-5214(01)00180-6)
8
9
10 327 11 Fan G, Zha J, Du R and Gao L, Determination of soluble solids and firmness of apples
11
12 328 by Vis/NIR transmittance. *J Food Eng* **93**: 416-420 (2009).
13
14 329 <https://doi.org/10.1016/j.jfoodeng.2009.02.006>
15
16
17 330 12 Ziosi V, Noferini M, Fiori G, Tadiello A, Trainotti L, Casadoro G and Costa G, A new
18
19 331 index based on vis spectroscopy to characterize the progression of ripening in peach
20
21 332 fruit. *Postharvest Biol Tec* **49**: 319-329 (2008).
22
23 333 <https://doi.org/10.1016/j.postharvbio.2008.01.017>
24
25
26 334 13 Bureau S, Ruiz D, Reich M, Gouble B, Bertrand D, Audergon JM and Renard CM,
27
28 335 Rapid and non-destructive analysis of apricot fruit quality using FT-near-infrared
29
30 336 spectroscopy. *Food Chem* **113**: 1323-1328 (2009).
31
32 337 <https://doi.org/10.1016/j.foodchem.2008.08.066>
33
34
35 338 14 Pérez-Marín D, Paz P, Guerrero JE, Garrido-Varo A and Sánchez MT, Miniature
36
37 339 handheld NIR sensor for the on-site non-destructive *J Food Eng* **99**: 294-302 (2010).
38
39 340 <https://doi.org/10.1016/j.jfoodeng.2010.03.002>
40
41
42 341 15 Munera S, Amigo JM, Blasco J, Cubero S, Talens P and Aleixos N, Ripeness
43
44 342 monitoring of two cultivars of nectarine using VIS-NIR hyperspectral reflectance
45
46 343 imaging. *J Food Eng* **214**: 29-39 (2017).
47
48 344 <https://doi.org/10.1016/j.jfoodeng.2017.06.031>
49
50
51 345 16 Li J, Huang W, Zhao C and Zhang B, A comparative study for the quantitative
52
53 346 determination of soluble solids content, pH and firmness of pears by Vis/NIR
54
55 347 spectroscopy. *J Food Eng* **116**: 324-332 (2013).
56
57 348 <https://doi.org/10.1016/j.jfoodeng.2012.11.007>
58
59
60

- 1
2
3 349 17 Goke A, Serra S and Musacchi S, Postharvest dry matter and soluble solids content
4
5 350 prediction in d'Anjou and Bartlett pear using near-infrared spectroscopy. *HortScience*,
6
7 351 **53**: 669-680 (2018). <https://doi.org/10.21273/hortsci12843-17>
9
10 352 18 Walsh KB, Long RL and Middleton SG, Use of near infra-red spectroscopy in
11
12 353 evaluation of source-sink manipulation to increase the soluble sugar content of
13
14 354 stonefruit. *J Hort Sci Biotech* **82**: 316-322 (2007).
15
16 <https://doi.org/10.1080/14620316.2007.11512235>
17
18 355
19 356 19 Golic M and Walsh KB, Robustness of calibration models based on near infrared
20
21 357 spectroscopy for the in-line grading of stonefruit for total soluble solids content. *Anal*
22
23 358 *Chim Acta* **555**: 286-291 (2006). <https://doi.org/10.1016/j.aca.2005.09.014>
24
25 359 20 Kaur H, Künnemeyer R and McGlone A, Comparison of hand-held near infrared
26
27 360 spectrophotometers for fruit dry matter assessment. *J Near Infrared Spec* **25**: 267-277
28
29 361 (2017). <https://doi.org/10.1177/0967033517725530>
30
31 362 21 Donis-González IR, Valero C, Momin MA, Kaur A and Slaughter DC, Performance
32
33 363 evaluation of two commercially available portable spectrometers to non-invasively
34
35 364 determine table grape and peach quality attributes. *Agronomy* **10**: 148 (2020).
36
37 <https://doi.org/10.3390/agronomy10010148>
38
39 365
40 366 22 HIN (Horticulture Industry Network). [Online]. Available:
41
42 367 <http://www.hin.com.au/networks/profitable-stonefruit-research/stonefruit-maturity->
43
44 368 [and-fruit-quality/da-meter-iad-maturity-classes-database](http://www.hin.com.au/networks/profitable-stonefruit-research/stonefruit-maturity-and-fruit-quality/da-meter-iad-maturity-classes-database) [30 November 2019]
45
46 369 23 Uwadaira Y, Sekiyama Y and Ikehata A, An examination of the principle of non-
47
48 370 destructive flesh firmness measurement of peach fruit by using VIS-NIR spectroscopy.
49
50 371 *Heliyon*, **4**: e00531 (2018). <https://doi.org/10.1016/j.heliyon.2018.e00531>
51
52 372 24 Minasny B and McBratney A Why you don't need to use RPD. *Pedomtron*, **33**: 14-15
53
54 373 (2013).
55
56
57
58
59
60

- 1
2
3 374 25 Louw ED and Theron KI. Robust prediction models for quality parameters in Japanese
4
5 375 plums (*Prunus salicina* L.) using NIR spectroscopy. *Postharvest Biol Tec*, **58**: 176-184
6
7 376 (2010). <https://doi.org/10.1016/j.postharvbio.2010.07.001>
8
9
10 377 26 Brizzolara S, Hertog M, Tosetti R, Nicolai B, Tonutti P. Metabolic responses to low
11
12 378 temperature of three peach fruit cultivars differently sensitive to cold storage. *Front*
13
14 379 *Plant Sci* **9**: 1-16 (2018). <https://doi.org/10.3389/fpls.2018.00706>
15
16
17 380 27 Travers S, Bertelsen MG, Petersen KK and Kucheryavskiy SV, Predicting pear (cv.
18
19 381 Clara Frijs) dry matter and soluble solids content with near infrared spectroscopy. *LWT-*
20
21 382 *Food Sci Tec* **59**: 1107-1113 (2014). <https://doi.org/10.1016/j.lwt.2014.04.048>
22
23
24 383
25
26
27
28
29
30
31
32
33
34
35
36
37
38
39
40
41
42
43
44
45
46
47
48
49
50
51
52
53
54
55
56
57
58
59
60

1
2
3 384 **Figure legends**
4

5 385

6
7
8 386 **Figure 1.** Fruit weight (FW, A), soluble solids concentration (SSC, B), flesh firmness (FF, C)
9
10 387 and dry matter concentration (DMC, D) in fourteen stone fruit cultivars at harvest
11
12 388 time (± 5 days). Boxplots display interquartile range boxes (1st to 3rd quartile), with
13
14 389 horizontal median lines, highest and lowest observations (whiskers) and outliers
15
16
17 390 (dots). Cultivar name abbreviations: 'Golden May' (GM), 'Angeleno' (AN), 'August
18
19 391 Bright' (AGB), 'Autumn Bright' (ATB), 'Rose Bright' (RB), 'September Bright' (SB),
20
21
22 392 'Ice Princess' (IP), 'Snow Fall' (SF), 'Snow Flame 23' (FL23), 'Snow Flame 25'
23
24 393 (FL25), 'August Flame' (AF), 'O'Henry' (OH), 'Redhaven' (RH) and 'September Sun'
25
26 394 (SS).
27

28 395

29
30 396 **Figure 2.** Coefficients of determination (R^2) and root mean square errors ($RMSE$) of partial
31
32
33 397 least square regression models for the prediction of soluble solids concentration
34
35 398 (SSC) with 1–10 principal components in the peach 'O'Henry'. Model and cross-
36
37 399 validation R^2 and $RMSE$ reported for the 729–975 nm absorbance (A and C) and for
38
39
40 400 its second derivative (B and D). Grey dashed vertical lines show the number of
41
42 401 principal components selected for SSC prediction.
43

44
45 402

46
47 403 **Figure 3.** Scatter plots of model and cross-validation (CV) prediction fits against actual
48
49 404 responses of soluble solids concentration (SSC). Dashed lines represent reference
50
51 405 linear fits where SSC prediction = SSC actual response. Cultivar name
52
53 406 abbreviations: 'Golden May' (GM), 'Angeleno' (AN), 'August Bright' (AGB),
54
55
56 407 'Autumn Bright' (ATB), 'Rose Bright' (RB), 'September Bright' (SB), 'Ice Princess'
57
58
59
60

1
2
3 408 (IP), 'Snow Fall' (SF), 'Snow Flame 23' (FL23), 'Snow Flame 25' (FL25), 'August
4
5 409 Flame' (AF), 'O'Henry' (OH), 'Redhaven' (RH) and 'September Sun' (SS).
6
7
8 410
9
10 411
11
12

13 412 **Figure 4.** Scatter plots of model and cross-validation (CV) prediction fits against actual
14
15 413 responses of dry matter concentration (DMC). Dashed lines represent reference
16
17 414 linear fits where DMC prediction = DMC actual response. Cultivar name
18
19 415 abbreviations: 'Golden May' (GM), 'Angeleno' (AN), 'August Bright' (AGB),
20
21 416 'Autumn Bright' (ATB), 'Rose Bright' (RB), 'September Bright' (SB), 'Ice Princess'
22
23 417 (IP), 'Snow Fall' (SF), 'Snow Flame 23' (FL23), 'Snow Flame 25' (FL25), 'August
24
25 418 Flame' (AF), 'O'Henry' (OH), 'Redhaven' (RH) and 'September Sun' (SS).
26
27
28
29 419
30

31 420 **Figure 5.** Scatter plots of model and cross-validation (CV) prediction fits against actual
32
33 421 responses of flesh firmness (FF). Dashed lines represent reference linear fits where
34
35 422 FF prediction = FF actual response. Cultivar name abbreviations: 'Golden May'
36
37 423 (GM), 'Angeleno' (AN), 'August Bright' (AGB), 'Autumn Bright' (ATB), 'Rose
38
39 424 Bright' (RB), 'September Bright' (SB), 'Ice Princess' (IP), 'Snow Fall' (SF), 'Snow
40
41 425 Flame 23' (FL23), 'Snow Flame 25' (FL25), 'August Flame' (AF), 'O'Henry' (OH),
42
43 426 'Redhaven' (RH) and 'September Sun' (SS).
44
45
46
47
48
49
50
51
52
53
54
55
56
57
58
59
60

Table 1. Partial least square regression model statistics for the prediction of soluble solids concentration (SSC), dry matter concentration (DMC) and flesh firmness (FF) using the 2nd derivative of the 729–975 nm absorbance.

Crop	Cultivar	Variable	PCs [†]	<i>RMSE</i> ^y	<i>RMSE</i> _{CV} ^x	<i>R</i> ^{2w}	<i>R</i> ² _{CV} ^v	<i>R</i> ² _{test} ^u	<i>n</i> _{train} ^t	<i>n</i> _{test} ^s	
Apricot	Golden	SSC	5	1.861	1.983	0.725	0.688	0.759	165	30	
		DMC	5	1.074	1.168	0.793	0.756	0.811	165	30	
	May	FF	5	1.272	1.379	0.581	0.508	0.438	165	30	
Plum	Angeleno	SSC	3	0.361	0.377	0.928	0.922	0.931	162	30	
		DMC	3	0.479	0.498	0.877	0.867	0.881	162	30	
		FF	3	0.442	0.459	0.225	0.163	0.336	162	30	
Nectarine	August	SSC	5	0.541	0.575	0.955	0.949	0.933	166	30	
		Bright	DMC	5	0.665	0.700	0.915	0.906	0.928	166	30
			FF	5	1.416	1.537	0.529	0.445	0.423	166	30
	Autumn	SSC	4	0.557	0.589	0.880	0.865	0.938	169	30	
		Bright	DMC	4	0.546	0.577	0.887	0.874	0.932	168	30
			FF	4	1.020	1.079	0.467	0.402	0.496	169	30
	Rose	SSC	5	0.574	0.614	0.939	0.930	0.919	166	30	
		Bright	DMC	5	0.602	0.650	0.914	0.900	0.954	166	30
			FF	5	1.327	1.399	0.499	0.443	0.000	166	30
	September	Bright	SSC	4	0.650	0.692	0.903	0.890	0.919	163	30
			DMC	4	0.647	0.695	0.914	0.901	0.945	163	30
			FF	4	0.989	1.032	0.449	0.399	0.177	162	30
White peach	Ice	SSC	3	0.715	0.755	0.918	0.909	0.922	164	30	
		DMC	3	0.640	0.683	0.930	0.920	0.786	164	30	
	Princess	FF	3	1.262	1.332	0.300	0.220	0.254	164	30	
		SSC	4	0.638	0.686	0.894	0.877	0.796	162	30	
	Snow Fall	DMC	4	0.712	0.767	0.876	0.856	0.844	162	30	
		FF	4	1.286	1.368	0.449	0.377	0.039	162	30	
Snow	SSC	5	0.761	0.812	0.892	0.877	0.865	160	30		

Yellow peach	Flame 23	DMC	5	0.683	0.734	0.900	0.884	0.862	160	30
		FF	5	0.908	0.971	0.567	0.505	0.580	160	30
		SSC	5	0.587	0.627	0.877	0.860	0.820	166	30
	Snow	DMC	5	0.502	0.542	0.891	0.872	0.824	166	30
		FF	5	0.940	0.991	0.625	0.583	0.656	165	30
		SSC	4	0.532	0.571	0.943	0.935	0.845	162	30
	August	DMC	4	0.598	0.643	0.909	0.895	0.864	163	30
		FF	4	1.287	1.363	0.459	0.393	0.488	161	30
		SSC	4	0.524	0.566	0.942	0.932	0.951	161	30
	OHenry	DMC	4	0.650	0.693	0.889	0.873	0.945	161	30
		FF	4	1.234	1.299	0.652	0.614	0.328	161	30
		SSC	4	0.570	0.606	0.790	0.762	0.754	167	30
	Redhaven	DMC	4	0.568	0.601	0.805	0.782	0.820	167	30
		FF	4	0.795	0.848	0.715	0.676	0.629	167	30
		SSC	5	0.637	0.683	0.913	0.900	0.945	162	30
	September	DMC	5	0.513	0.558	0.943	0.932	0.923	162	30
		FF	5	1.187	1.237	0.459	0.383	0.208	162	30
		SSC	5	0.637	0.683	0.913	0.900	0.945	162	30
Sun	DMC	5	0.513	0.558	0.943	0.932	0.923	162	30	
	FF	5	1.187	1.237	0.459	0.383	0.208	162	30	
	SSC	5	0.637	0.683	0.913	0.900	0.945	162	30	

^zNumber of principal components; ^yroot mean square error (*RMSE*) of the model; ^x*RMSE* of the cross-validation; ^wcoefficient of determination (R^2) of the model; ^v R^2 of the cross-validation; ^u R^2 of the validation test; ^ttrain-sample size and ^stest-sample size.

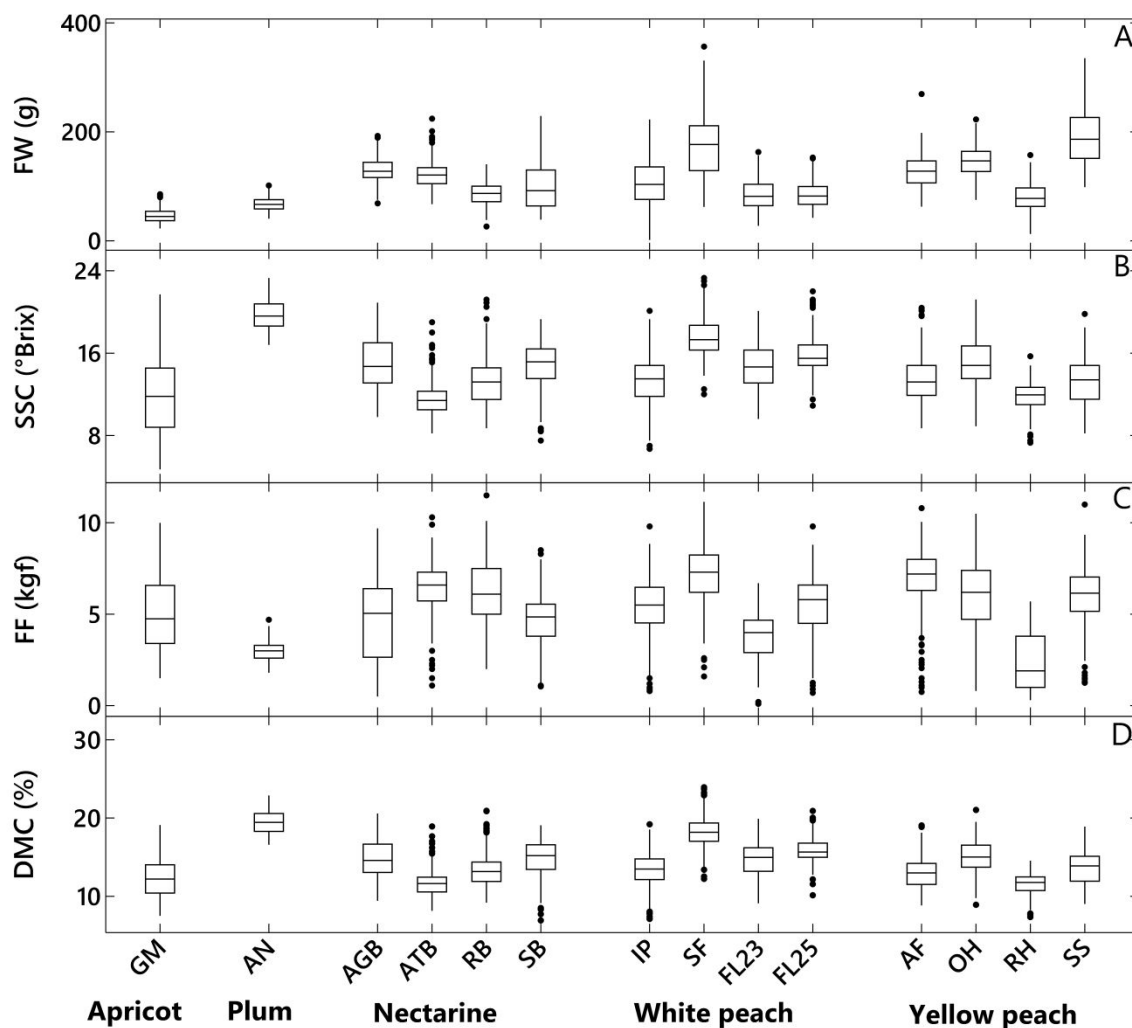


Figure 1. Fruit weight (FW, A), soluble solids concentration (SSC, B), flesh firmness (FF, C) and dry matter concentration (DMC, D) in fourteen stone fruit cultivars at harvest time (± 5 days). Boxplots display interquartile range boxes (1st to 3rd quartile), with horizontal median lines, highest and lowest observations (whiskers) and outliers (dots). Cultivar name abbreviations: 'Golden May' (GM), 'Angeleno' (AN), 'August Bright' (AGB), 'Autumn Bright' (ATB), 'Rose Bright' (RB), 'September Bright' (SB), 'Ice Princess' (IP), 'Snow Fall' (SF), 'Snow Flame 23' (FL23), 'Snow Flame 25' (FL25), 'August Flame' (AF), 'O'Henry' (OH), 'Redhaven' (RH) and 'September Sun' (SS).

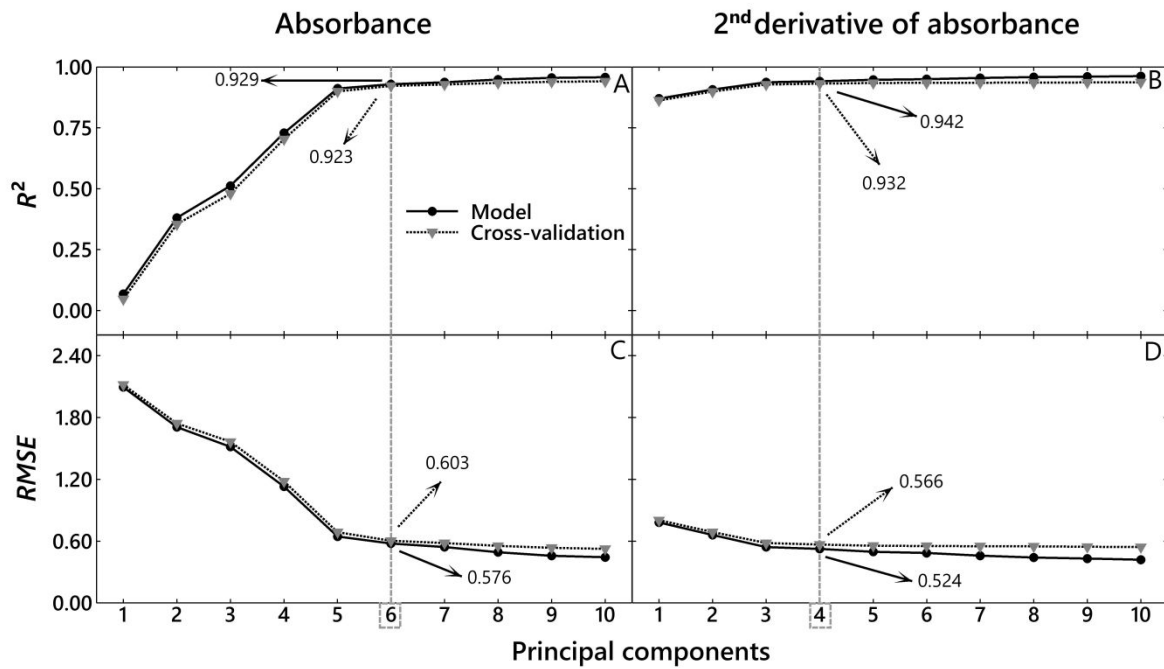


Figure 2. Coefficients of determination (R^2) and root mean square errors ($RMSE$) of partial least square regression models for the prediction of soluble solids concentration (SSC) with 1–10 principal components in the peach 'O'Henry'. Model and cross-validation R^2 and $RMSE$ reported for the 729–975 nm absorbance (A and C) and for its second derivative (B and D). Grey dashed vertical lines show the number of principal components selected for SSC prediction.

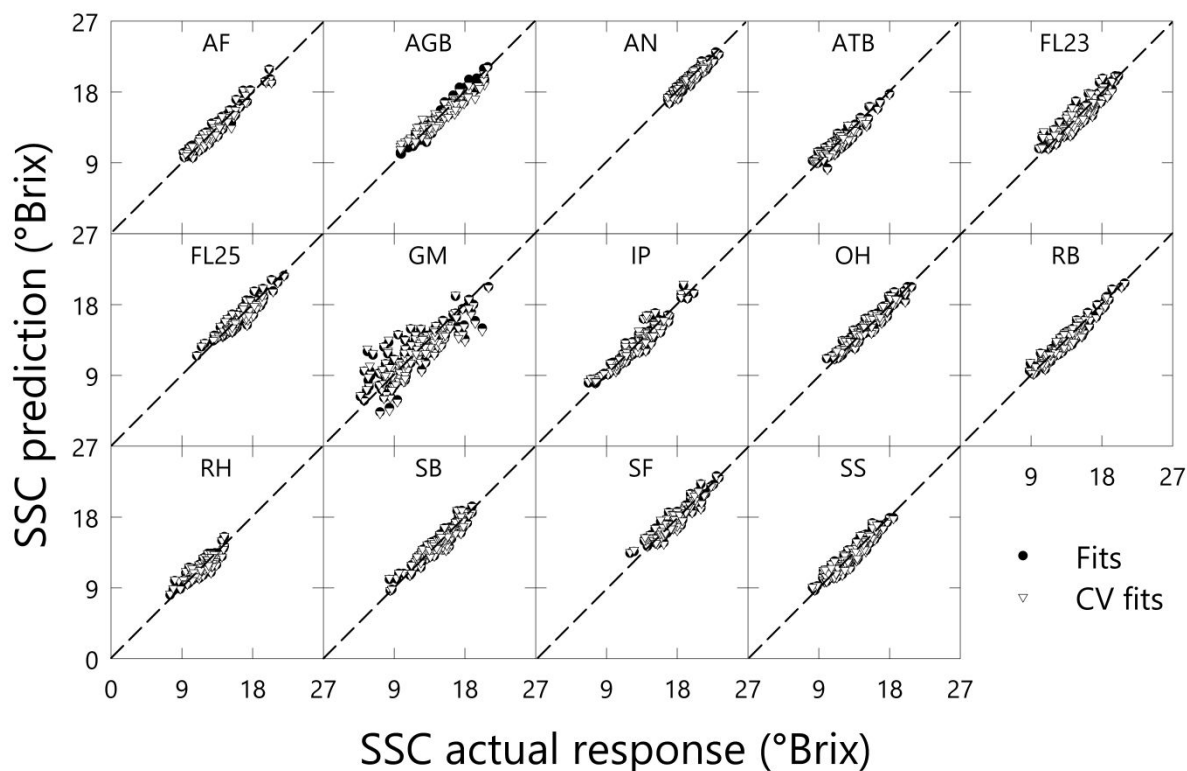


Figure 3. Scatter plots of model and cross-validation (CV) prediction fits against actual responses of soluble solids concentration (SSC). Dashed lines represent reference linear fits where $\text{SSC prediction} = \text{SSC actual response}$. Cultivar name abbreviations: 'Golden May' (GM), 'Angeleno' (AN), 'August Bright' (AGB), 'Autumn Bright' (ATB), 'Rose Bright' (RB), 'September Bright' (SB), 'Ice Princess' (IP), 'Snow Fall' (SF), 'Snow Flame 23' (FL23), 'Snow Flame 25' (FL25), 'August Flame' (AF), 'O'Henry' (OH), 'Redhaven' (RH) and 'September Sun' (SS).

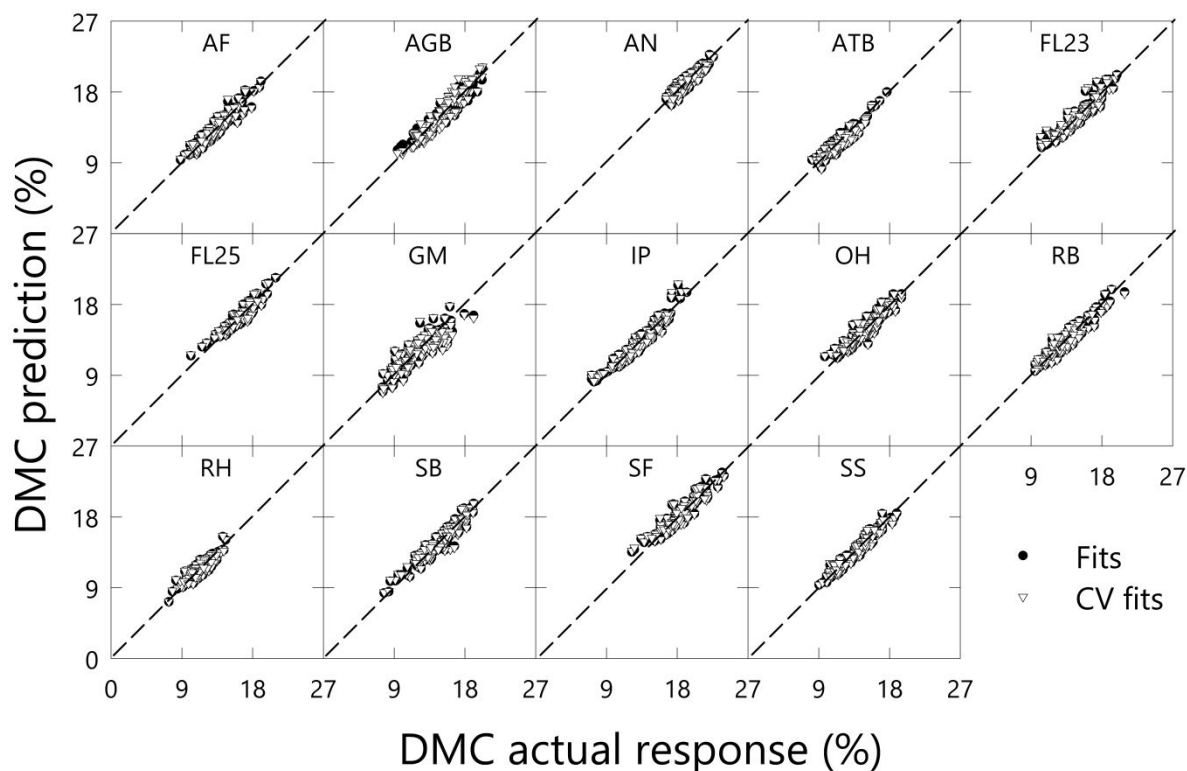


Figure 4. Scatter plots of model and cross-validation (CV) prediction fits against actual responses of dry matter concentration (DMC). Dashed lines represent reference linear fits where DMC prediction = DMC actual response. Cultivar name abbreviations: 'Golden May' (GM), 'Angeleno' (AN), 'August Bright' (AGB), 'Autumn Bright' (ATB), 'Rose Bright' (RB), 'September Bright' (SB), 'Ice Princess' (IP), 'Snow Fall' (SF), 'Snow Flame 23' (FL23), 'Snow Flame 25' (FL25), 'August Flame' (AF), 'O'Henry' (OH), 'Redhaven' (RH) and 'September Sun' (SS).

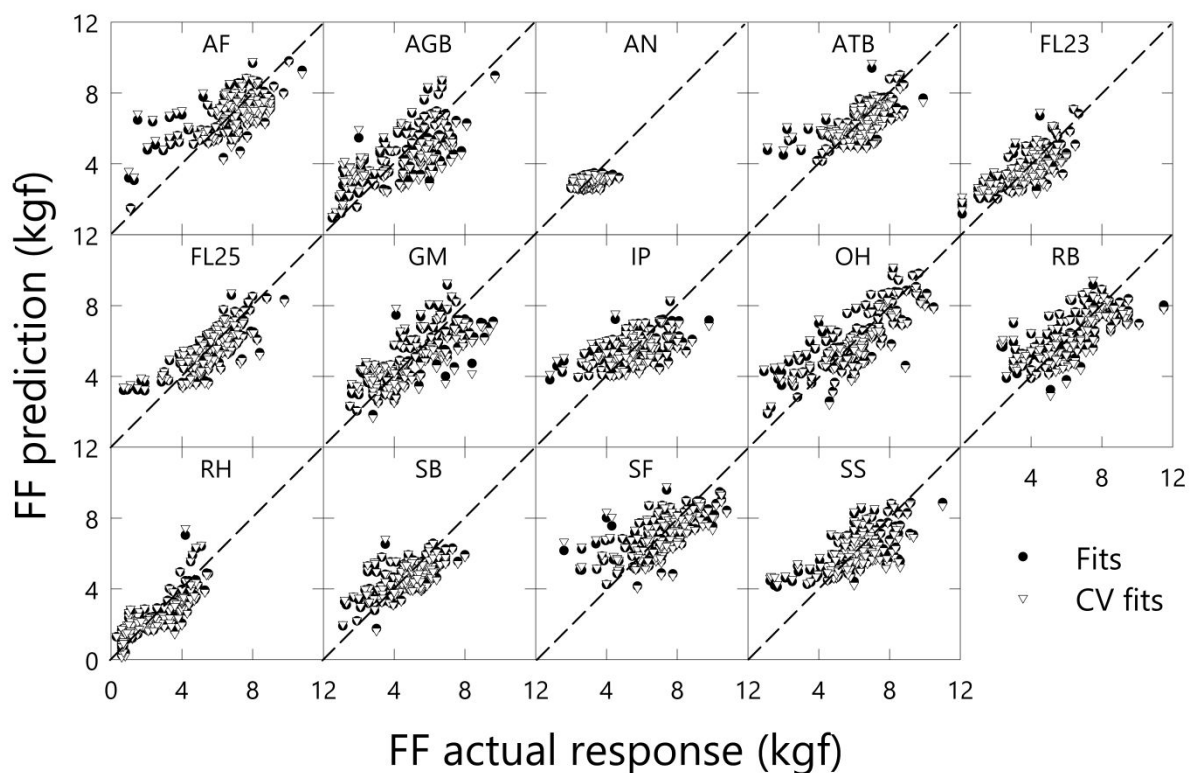


Figure 5. Scatter plots of model and cross-validation (CV) prediction fits against actual responses of flesh firmness (FF). Dashed lines represent reference linear fits where FF prediction = FF actual response. Cultivar name abbreviations: 'Golden May' (GM), 'Angeleno' (AN), 'August Bright' (AGB), 'Autumn Bright' (ATB), 'Rose Bright' (RB), 'September Bright' (SB), 'Ice Princess' (IP), 'Snow Fall' (SF), 'Snow Flame 23' (FL23), 'Snow Flame 25' (FL25), 'August Flame' (AF), 'O'Henry' (OH), 'Redhaven' (RH) and 'September Sun' (SS).